



Mechanical Properties of Nano SiC Reinforced Aluminum 7075-T6 Produced by Warm Powder Compaction using an Inert Gas

G.H. Majzoobi¹, T. Torkeman¹

¹Mechanical Engineering Department, Bu-Ali Sina University, Hamedan, Iran

PAPER INFO

Paper history:

Received 11 July 2023
Received in revised form 30 July 2023
Accepted 30 July 2023

Keywords:

Nano-composite; Aluminum 7075-T6; Powder compaction; SiC particle.

ABSTRACT

The micron-sized Al7075 powder reinforced with nano-sized SiC particles is compacted at 400°C in an inert atmosphere using Nitrogen. It is shown that this technique can significantly improve the mechanical properties of the compacted powder characterized by hardness measurement, stress-strain curves and density. The maximum relative density was %98.8 for 2.3 GPa pressure and 0%SiC content. The minimum density was %93.95 for 10%SiC content and 1.3 GPa pressure. The degree of porosity and the number and size of the void decreased with the increase of the compaction pressure and increased with the increase of SiC volume fraction. The maximum improvement of the ultimate strength was about 72% and occurred for the 5%SiC content and the 1.3 GPa compaction pressure. For 10%SiC volume fraction the strength improved by 53% for 2.6 GPa pressure. The effect of SiC content on ultimate strength was significantly higher than that of the compaction pressure. 100% increase in Vickers hardness obtained for the samples with 10%SiC volume fraction, compacted at 2.6 GPa pressure. Again, the effect of SiC volume fraction on hardness improvement was found to be remarkably greater than that of compaction pressure.

1. INTRODUCTION

Aluminum alloys usually have a high strength to weight ratio and have wide application in various industries [1, 2, 3]. Among the aluminum alloys, Al7075 has gained wide applications over the past decades. This is due to its mechanical properties which are comparable with some of steel alloys [4]. By reinforcing such alloys with ceramic nano particles such as SiC, Al₂O₃, B₄C, and TiB₂ through powder metallurgy (PM) aluminum-matrix nanocomposites (AMNC) can be produced with higher mechanical properties [5]. Aluminum matrix composites (AMC) are widely used in aerospace, automotive, military and micro electronics industries because of their superior properties such as wear resistance and strength-to-weight ratio.

The powder compaction can be performed by different techniques [6, 7, 8]. The first technique which is based on green density comprises cold powder compaction followed by hot sintering. In the second technique, the compaction is performed using pressure and temperature at the same time to reach a full density.

By adding ceramic powders to aluminum and mechanical milling, the ceramic particles are dispersed in the matrix and cause the reduction of grains and dislocation interlocking within the matrix. This in turn enhances the mechanical

properties of the composite. The mechanical alloying is performed through high energy ball milling in which the particles are impacted by high energy and then are cold sintered [9]. The high energy ball milling also gives rise to uniform dispersion of the reinforcing particles within the matrix and prevent agglomeration which is detrimental to production of nanocomposites.

Different PM techniques based on thermo-mechanical processes can be used for preparation of particulate reinforced nanocomposites. In all of these techniques, the load can be applied either quasi-statically or dynamically. Hot pressing [10], hot isostatic pressing (HIP) [11] and hot extrusion [12] are typical examples of quasi-static loading.

Hubi Haleem et al [13] studied Brinell hardness (BHN) and compression strength of aluminum matrix composite material that reinforced by (3, 6, 9, and 12 wt.%) Al₂O₃ particles using powder technology and prepared the samples by using single action pressing then followed directly by sintering process at 500°C under the effect of inert gas conditions. The increase in the Brinell hardness (BHN) and compression strength were found to reach 89% and 54%, respectively.

Ramesh et al [14] evaluated the effect of the workability behaviour of pure Aluminium and Al 20% SiC powder metallurgy composites introducing various sizes of the second phase particles. Kalkanli and Yilmaz [15] used pressure

*Corresponding Author Email: gh_majzoobi@basu.ac.ir
(Prof. G.H. Majzoobi)

casting for producing composites of 7075 matrix alloy and SiC particles. The maximum flexural strength increased by about 40 MPa (10%) for the as-cast and 180 MPa (44%) for heat treated composites. For the as-cast specimens the hardness values increased from 133 to 188 Vickers with an increase in SiC content from 0 to 30 wt% and for the heat treated specimens the hardness increased from 171 to 221 Vickers. Taleghani et al [16] studied the hot deformation behaviour of 7075 aluminium alloy powder compacts with relative green densities ranging from 83 to 95%, at temperatures ranging from 350 °C to 450 °C and at true strain rates ranging from 0.01 s⁻¹ to 10 s⁻¹. As the deformation temperature increased or the strain rate and green density decreased, a decrease in the peak stress level was observed. Kumar et al [16] evaluated the effect of different percentage of Glass on workability behavior of Al-Glass composite in Powder metallurgy. The glass as reinforcement varied from 0% to 8% with particle size of 60 μm. It was found that a the workability parameter increased as the percent content of Glass increased. Majzoobi et al [17] investigated the wear resistance of Al7075-SiC nanocomposite prepared by hot dynamic compaction. Majzoobi et al [18] studied the hot quasi-static pressing and dynamic compaction of Al7075-B4C composite powder. Atrian *et al.* [19] compared dynamic compaction and hot pressing techniques in processing and characterization of Al7075-SiC nanocomposite.

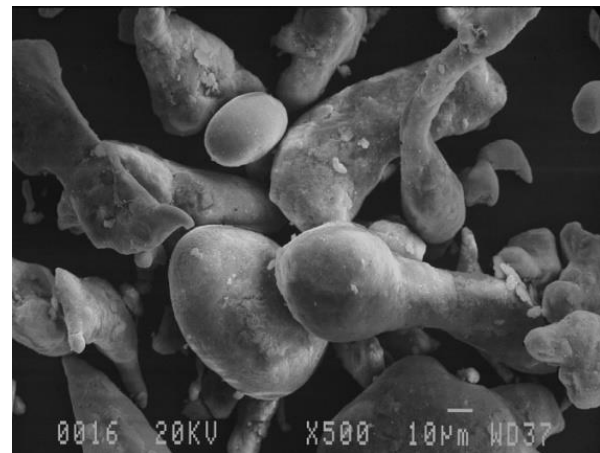
As stated above, the composites can also be produced under dynamic compaction [17, 18] or shock wave consolidation [19]. These techniques usually use dropping hammer, explosives or compressed gas as the propellant to accelerate a projectile for compaction. The main advantage of these types of production techniques is that hot sintering is usually (but not always) eliminated from the production cycle. Such techniques offer the possibility of producing the high temperatures necessary for adequate local metallurgical bonding at the powder particle interfaces, precisely where it is required, while the powder remains relatively cool elsewhere. Therefore, the microstructural changes such as particles agglomeration and grains growth which may happens due to high temperature rise, can be minimized [20]. Rahmani et al. [21] investigated the effect of compaction velocity, size, and content of reinforcing particles on corrosion resistance of Mg-B4C composites. For further details about the effects of strain rate or loading rate on powder compaction the readers are referred to references [22-24].

In the current work, Al7075-SiC nanocomposite is fabricated by mechanical milling and hot compaction in an inert atmosphere. The main objective of this study is to explore the aspects of nano particles reinforced Al7075. Moreover, the effect of volume fraction of nano reinforcement on density, compressive stress-strain curve, micro-hardness, and microstructural behavior of the specimens are investigated.

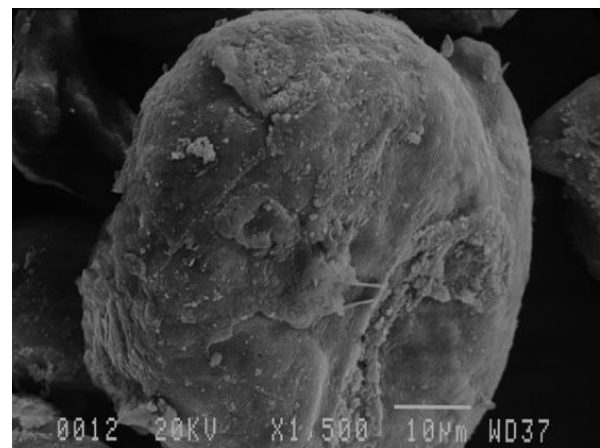
2. MATERIAL

The as-received materials were Al7075-T6 (gas atomized, - 100 μm , irregular morphology, Khorasan Powder Metallurgy Co., Iran) and SiC (average 50 nm , purity > 99.0%, specific surface area > 90 m² / g , nearly spherical morphology). The Al/SiC composites reinforced by 5 and 10% of SiC were prepared by mixing manually the two materials. The mixture

was then suspended in ethanol and was vibrated through ultrasonic process for 20 minutes in order to avoid particles agglomeration and to achieve a more uniform dispersion of nano particles. After drying, the mixture was milled in a planetary ball mill at room temperature and in an inert nitrogen atmosphere. The milling device contained twenty-two 10 mm diameter hard chromium steel balls embedded in a 125 ml volume steel vial. In order to have ball-to-powder mass ratio 3:1, thirty g of the powder mixture was milled at a rotation speed of 300 rpm for 2 hours. 0.5 wt.% of stearic acid was also added as process control agent (PCA). The morphology of the as-received Al7075 powder and the milled mixtures is illustrated in Fig. (1). Fig. 1(b) indicates that the SiC nano particles have fully covered the surface of Al7075 micron-sized particles after mechanical milling. Fig. 1(a) depicts distribution of some aluminum particles with irregular shapes. The agglomeration of SiC nano particles is clearly seen in Fig. 2 in form of the white spots. As observed in Fig. 2(b) agglomeration is higher for the 10%SiC volume fraction.

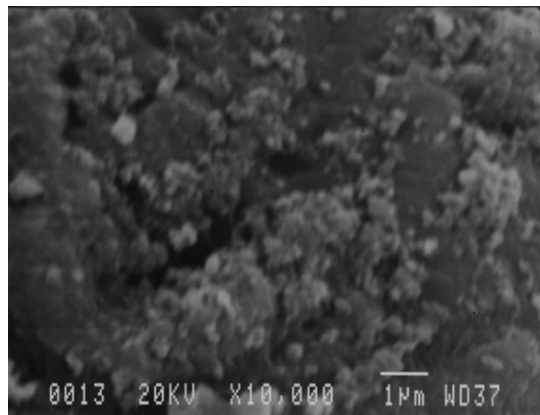


(a)

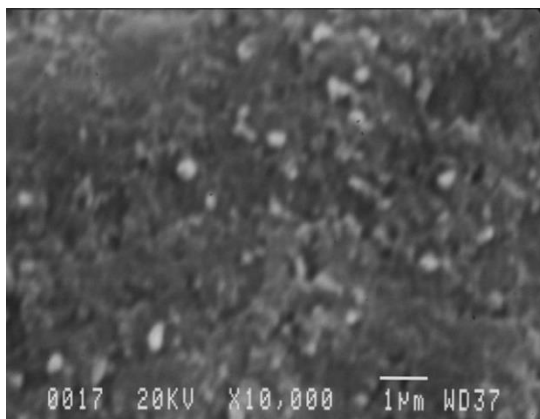


(b)

Fig. 1: Morphology of the as-received Al7075 powder and the milled mixture with two different magnifications.



(a)



(b)

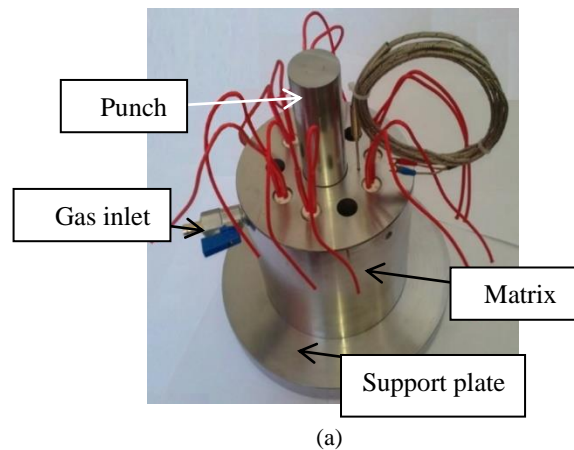
Fig. 2: SEM pictures showing the distribution of SiC nano particles on aluminum micro-sized particles for (a) 5% and (b) 10% SiC.

3. COMPACTION DIE AND TEST PROCEDURE

A general view of the die assembly used for compaction of the composites is shown in Fig. 3(a). The exploded view of the die is illustrated in Fig. 3(b). The parts numbered in the figure are: (1) general view of the matrix, (2) the conical section of the matrix, (3) the conical step beneath the matrix, (4) the matrix support plate, (5) the mandrel for compacting the powder and (6) the upper mandrel. The die assembly consisted of the die mold (made of steel 2713), die punch (made of steel 2344), heating elements and Nitrogen gas duct. The Nitrogen gas duct was to convey the gas into the die during the process of compaction to prevent the aluminum particles from oxidation. The die was designed using the software CATIA [25]. The model is shown in Fig. 4. This was to ensure that the die elements could withstand the pressures of compaction required to reach the highest density. Three pressures of 1.3, 1.95 and 2.3 GPa were considered for compaction in this work. The pressures designated here lie within the range of pressures which have been reported in the literature. The composite powders were compacted on a 400 tones hydraulic press. The loads required to produce the pressures 1.3, 1.95 and 2.3 GPa were 150, 225 and 300 tones, respectively. The compactions were conducted at 400°C which was roughly 80% of

Aluminum 7075 melting temperature, 477°C. The test procedure was as follows:

- 1- Twenty five grams of the composite powder was poured in the die container (matrix).
- 2- The punch was pushed into the matrix as far as 1 cm to seal the container against gas leakage.
- 3- Nitrogen was injected into the container for two minutes. This time was enough to discharge the oxygen from the container. The injection of Nitrogen continued to the end of the compaction process.
- 4- The heating of the die started and continued until the temperature of the powder reached the sintering temperature, 400°C. The temperature remained unchanged during the process of compaction.
- 5- The composite powder was compacted while Nitrogen was flowing through the container and temperature was 400°C.



(a)



(b)

Fig. 3: (a) A general view of the die assembly and (b) different parts of the die

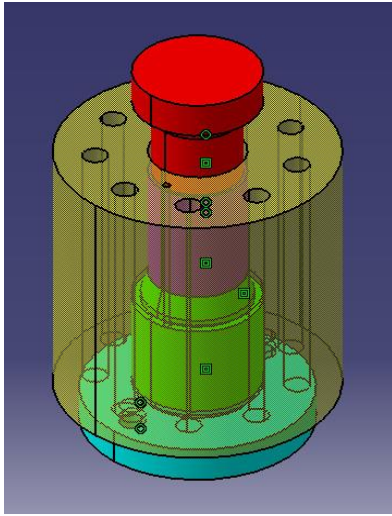


Fig. 4: The die assembly modeled by CATIA software

4. RESULTS AND DISCUSSION

The density, stress-strain curve and hardness of the compacted specimens were studied in this work. The reason is that these three parameters can well characterize the materials produced by powder compaction technique.

4.1 COMPACT DENSITY

Relative density was used to study the effect of SiC on the compact density in this work. Relative density is defined as the ratio of the green density of the compacted powder and the theoretical density of aluminum-7075 in solid state. The green density is also the density of the compacted powder before sintering. For instance, the theoretical density of aluminum 7075 containing 10% SiC particles is:

$$0.1 \times 3.2 + 0.9 \times 2.81 = 2.849 \text{ g/cm}^3$$

Where the theoretical densities of aluminum and SiC are 2.81 and 3.2 gr/cm³ respectively. In order to increase the accuracy of green density measurement, the Archimedes principal was used to measure the density of consolidated samples. In order to study the effect of SiC volume fraction on mechanical properties of Al7075-SiC composite, specimens with different contents of nano silicon carbide, 0, 5, and 10 vol%, were prepared under the pressures of 1.3, 1.95 and 2.3 GPa. Variations of relative density versus the volume fraction of SiC and the compaction pressure are depicted in Fig. 5 and are given in Table 1. The maximum relative density is %98.8 obtained for 2.3 GPa pressure and 0%SiC content. The minimum density is %93.95 obtained for 10%SiC content and 1.3 GPa pressure. As it is seen in Table 1, the increase of compaction pressure gives rise to the increase of relative density, as expected. The maximum increase is 1.4 and occurs for 2.3 GPa pressure. However, adding the reinforcing SiC particles to aluminum powder exhibits opposite effect and reduces the relative density. The maximum reduction in density is 1.8 and occurs for 10%SiC content.

Table 1: The variation of relative density due to SiC volume fraction and compaction pressure

| P(GPa) | Density reduction From 0 to 5%SiC | Density reduction From 0 to 10%SiC |
|--------|---|---|
| 1.3 | 1.2 | 2.6 |
| 1.95 | 1 | 2.35 |
| 2.3 | 1.4 | 2.57 |
| SiC% | Density increase (%) From 1.3 to 1.95 GPa | Density increase (%) From 1.3 to 1.95 GPa |
| 0 | 0.8 | 1.8 |
| 5 | 1 | 1.5 |
| 10 | 1 | 1.8 |

In general, compaction and sintering of composites are different from those of mono phase materials. The presence of hard and non-deformable particles such as SiC in a ductile matrix such as aluminum reduces its pressability. The reduction, however, increases for higher volume fraction of reinforcing particles.

4.2 SEM EXAMINATION

SEM pictures of the microstructure of three samples produced under different compaction pressures and 0%SiC are illustrated in Fig. 6. As the figure indicates, the degree of porosity and the number and size of the void decreases as the compaction pressure increases. The best compaction and the minimum porosity is seen in Fig. 6(c) for the 2.6GPa compaction pressure. In Fig. 6(c), the aluminum particles are completely interlocked with no porosity or void in between. The micrograph of a 0%SiC specimen with magnification of 2500 is depicted in Fig. 6(d). As the figure indicates, many pores are homogeneously dispersed on the aluminum particle seen in the figure. In the SiC particles reinforced samples, the porosity increases with the increase of SiC volume fraction. In the SiC reinforced samples, the fine nano-size SiC particles are easily pushed into pores among the coarse micro-size aluminum particles leading to reduction of porosity and to the increase the green density. Furthermore, plastic deformation due to localized heat generated by friction and displacement of powder particles gives rise to softening or melting layer which in turn enhance the bonding between particles and leading again to the increase of green density [26].

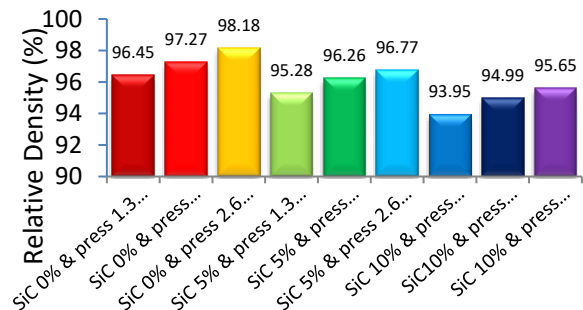
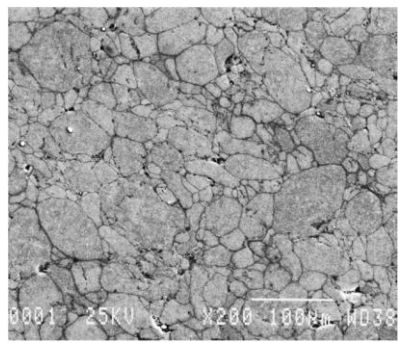
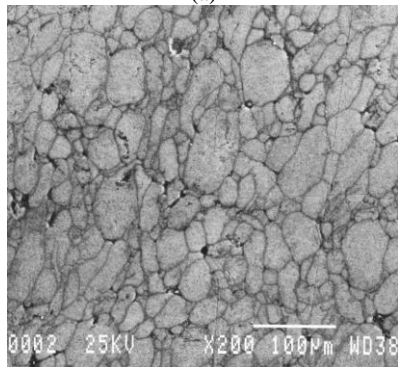


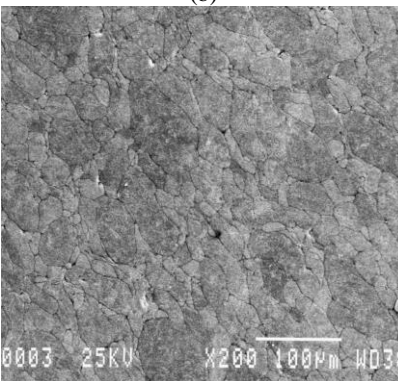
Fig. 5: Variation of relative density versus volume fraction of SiC and press pressure.



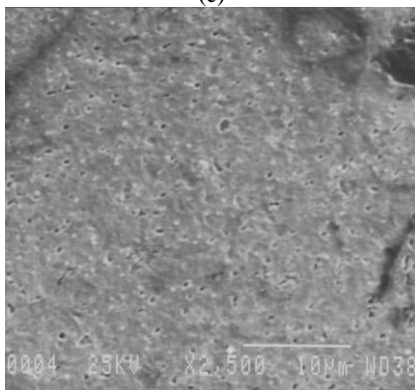
(a)



(b)

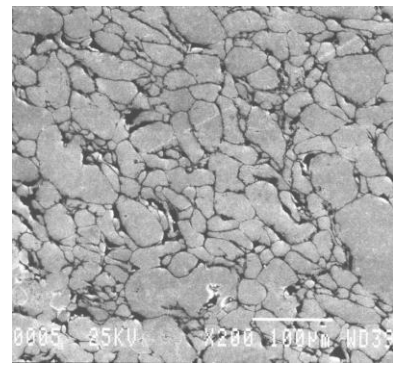


(c)

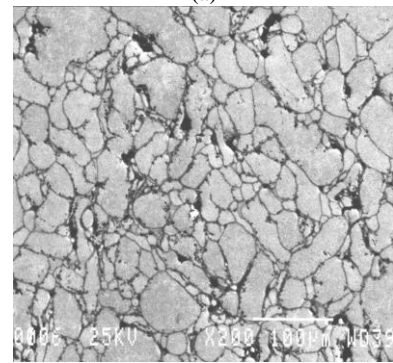


(d)

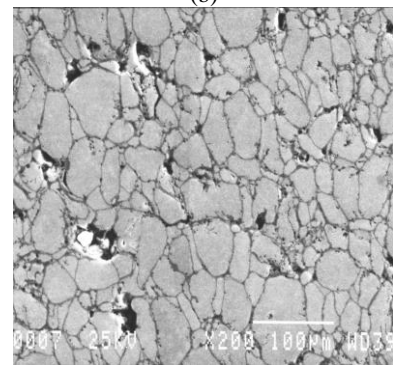
Fig. 6: SEM pictures of samples taken for different compression pressures and 0% SiC . (a) 0% SiC, (b) P=1.3GPa, SiC=0%, (c) P=1.95GPa, SiC=0%, (d) P=2.6GPa, SiC=0% and Magnification =2500



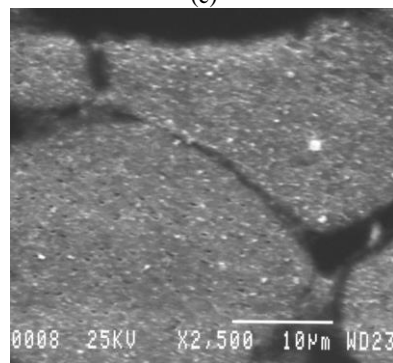
(a)



(b)



(c)



(d)

Fig. 7: SEM pictures of samples produced under different compression pressures and 5% SiC. (a) P=1.3GPa, SiC=5% , (b) P=1.95GPa, SiC=5%, (c) P=2.6GPa, SiC=5%, (d) SiC=5%, Magnification =2500

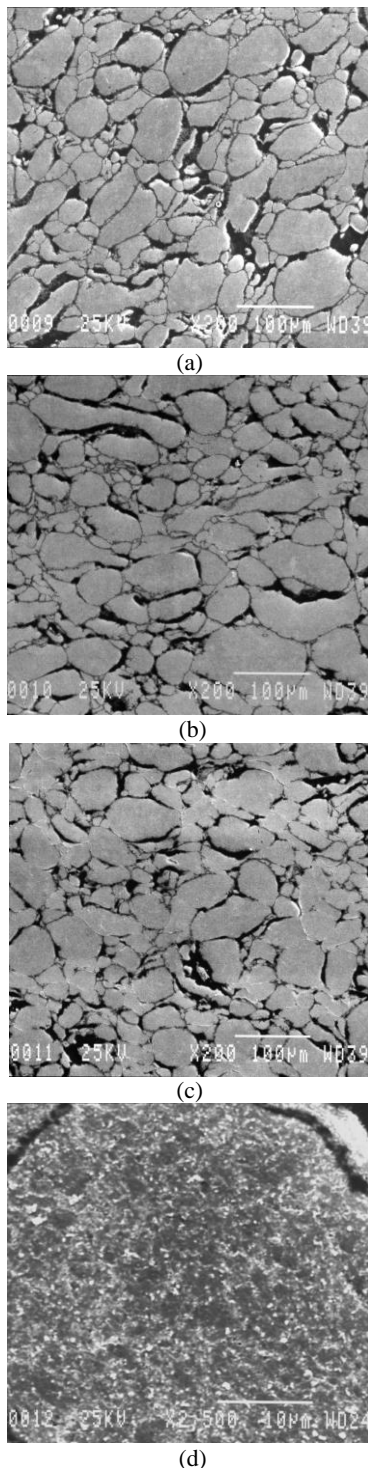


Fig. 8: SEM pictures of samples produced under different compression pressures and 10% SiC, (a) P=1.3GPa, SiC=10%, (b) P=1.95GPa, SiC=10%, (c) P=2.6GPa, SiC=10%, (d) SiC=10%, Magnification =2500

Figs. 7(d) and 8(d) show nano SiC particles settled on aluminum particle and at the boundary of adjacent aluminum particles. The EDS point analysis also confirms that the dispersed particles at the boundary are SiC. These hard and stiff nano particles, weaken the bonding of Al micron-sized particles. As a result, more pores remain within the samples. This type of behavior for relative density versus the volume fraction of reinforcing particles has been reported frequently in the literature. Rahimnejad Yazdi et. al. [27] reported that relative density of Alumina/SiC nanocomposites decreased with the increase of SiC content. They attributed this attitude to the poor sinterability of SiC at temperatures normally used to sinter aluminum. Dong et al [28] also attributed this behavior to the incorporation of reinforcing particles that block grain boundary movement and hinder the densification of matrix material.

In order to observe the effect of increased percent of Silicon Carbide on grain boundaries of the compacted specimens, the SEM pictures shown individually in Figs. 6 to 8 are collectively compared in Fig. 9.

4.3 STRESS-STRAIN CURVES OF COMPACTS

The 12mm thick specimens were cut out, for compression test, from the compacted samples. Nine specimens with three different SiC volume fractions and compacted at three compaction pressures of 1.3, 1.95 and 2.6 GPa were prepared for nine compression tests. The samples prepared by wire cutting technique are shown in Fig. 10. The stress-strain curves of the specimens with the same SiC volume fractions for various compaction pressures are illustrated in Fig. 11. The increase in ultimate strength of the samples with respect to the strength of the specimen compacted at 1.3 GPa pressure is illustrated in Fig. 12. As the figure suggests, the maximum increase is about 17% and has occurred for the 0%SiC content and the 2.6 GPa compaction pressure. For 10%SiC volume fraction the strength improvement is nearly zero for 1.95 GPa pressure and only 4% for the 2.6GPa pressure. This implies that the compaction pressure is not so influential on the strength of powder compact.

The stress-strain curves of the specimens compacted at the same pressure for various SiC volume fractions are illustrated in Fig. 13. The increase in ultimate strength of the compactions with respect to the strength of the compact with 0%SiC volume fraction is illustrated in Fig. 14. As the figure suggests, the maximum increase is about 72% and occurs for the 5%SiC content and the 1.3 GPa compaction pressure. For 10%SiC volume fraction the strength improves by 53% for 2.6 GPa pressure. This implies that the SiC volume fraction is significantly influential on the strength of powder compact. A comparison between the Figs. 12 and 14 reveals that the effect of SiC content on ultimate strength is remarkably higher than that of the compaction pressure.

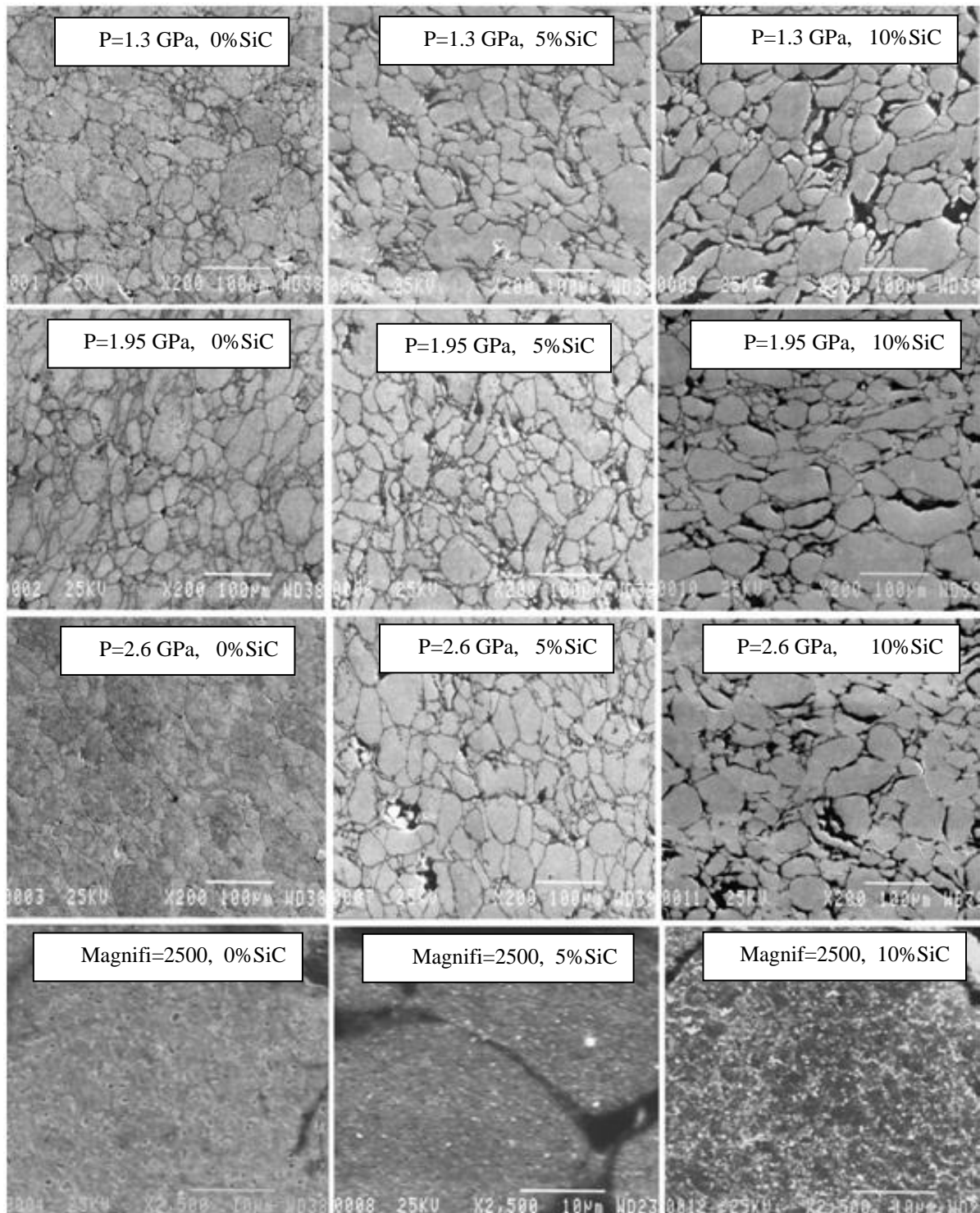


Fig. 9: A comparison between the SEM pictures of specimens for various pressures and SiC volume fraction (Magnifi stands for magnification)

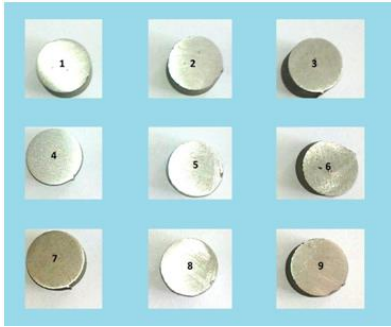
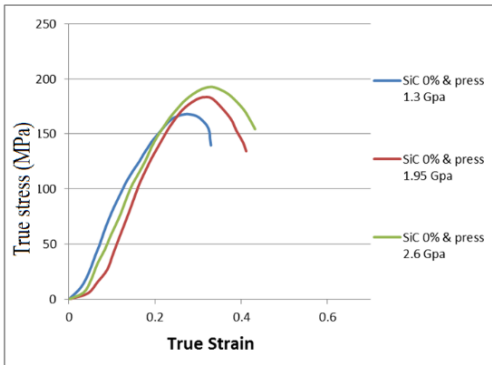
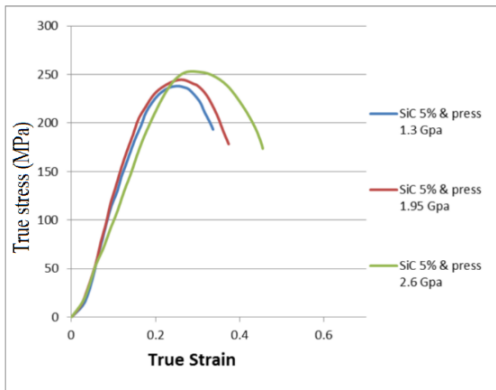


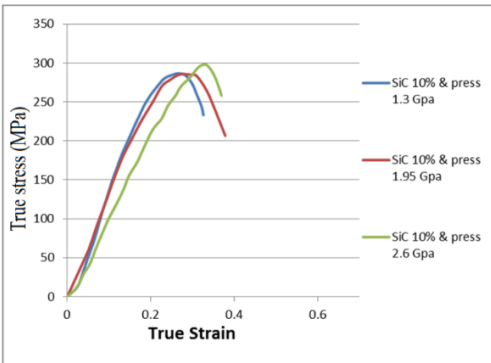
Fig. 10: Nine samples prepared by wire cutting technique for compression test



(a) 0%SiC



(b) 5%SiC



(c) 10% SiC

Fig. 11: Stress-strain curves of the samples with similar SiC fraction for the compaction pressures of 1.3, 1.95 and 2.6 GPa

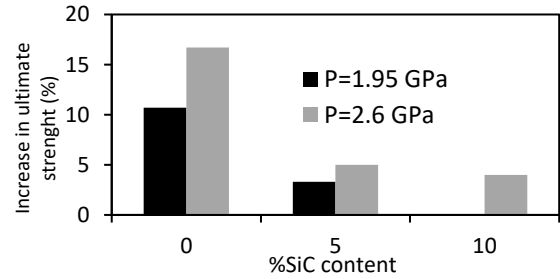
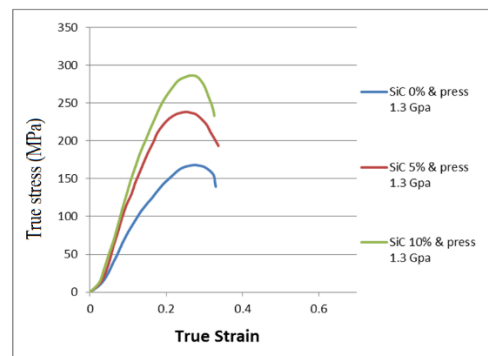
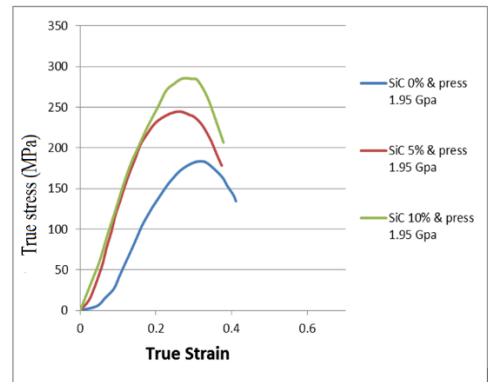


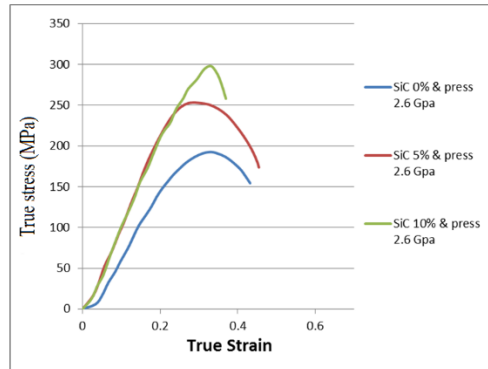
Fig. 12: The increase in ultimate strength of the compactions with respect to 1.3 GPa compaction pressure



(a) P=1.3 GPa



(b) P=1.95 GPa



(c) P=2.6 GPa

Fig. 13: Stress-strain curves of the samples with 0%SiC, 5%SiC and 10%SiC for the same compaction pressures level

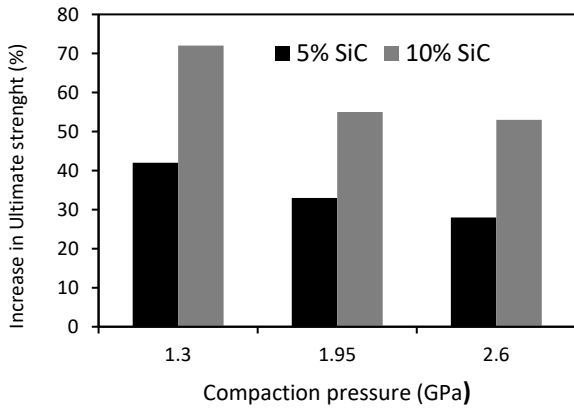


Fig. 14: The increase in ultimate strength of the compactions with respect to 0%SiC volume fraction

As it is seen, the micron-sized Al7075 powder reinforced with nano-sized SiC particles and compacted at 400°C in an inert atmosphere using Nitrogen leads to significant improvement in ultimate strength of the resulting composite. On the other hand, it is well-known that material endurance fatigue limit varies with ultimate strength level as shown in Figure 15 [29, 30]. Therefore, it can be concluded that the improvements made in this study in ultimate strength of aluminum 7075/SiC composite can also give rise to improvement in fatigue life of the composite as well.

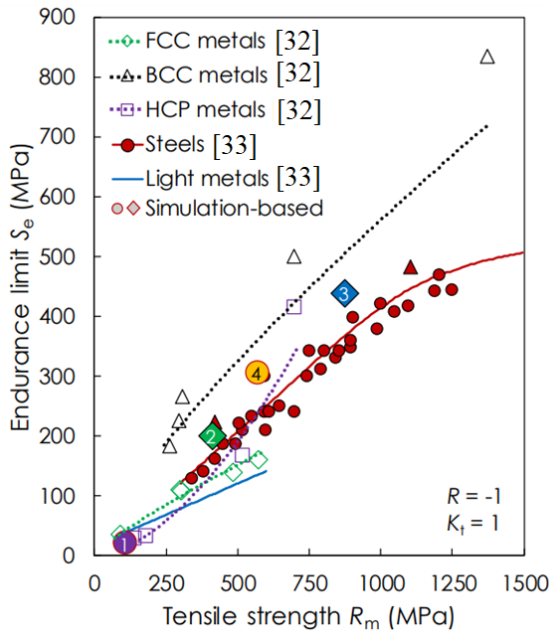


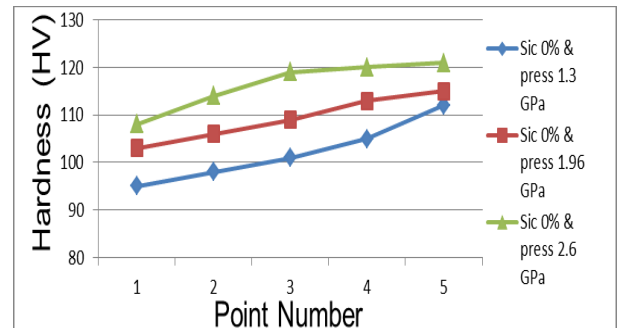
Figure 15: Relation between fatigue endurance limit, S_e , and ultimate strength, R_m , for various metals [29, 30]

4.4 HARDNESS MEASUREMENT

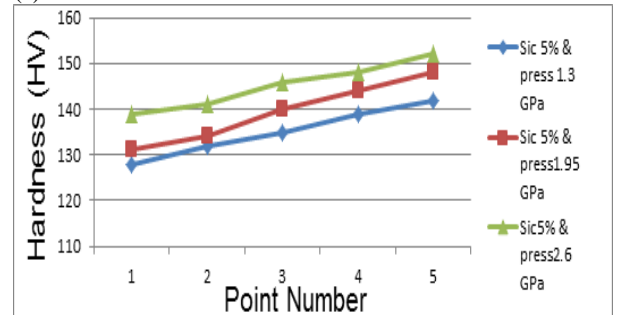
Enhancement of hardness is directly related to improvement of material strength. Therefore, hardness measurement is

always used as a tool for evaluation of powder compact quality. In this work, Vickers and Brinell standards were used for hardness measurement.

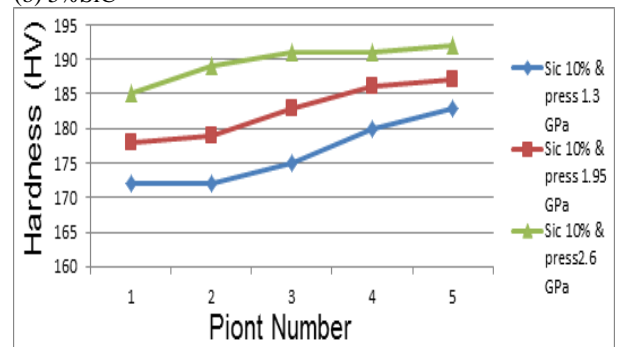
Because of nonuniformity of density of the compacted samples, hardness was measured at five different points. Variation of Vickers hardness at 5 points on the samples with similar SiC content and for different compaction pressures is illustrated in Fig. 16. As the figure suggests, hardness increases considerably with compaction pressure and SiC content. Variation of Vickers hardness for samples with different SiC contents and the same compaction pressure is illustrated in Fig. 17. In fact, despite of reduction of density with the increase of SiC content, the nano reinforcement could enhance the hardness. The latter is speculated to be due to second-phase hardening effects of added nanophase and its intrinsic hardness. Similar observations have already been reported by Canakci [31] and Alizadeh et. al. [32].



(a) 0%SiC

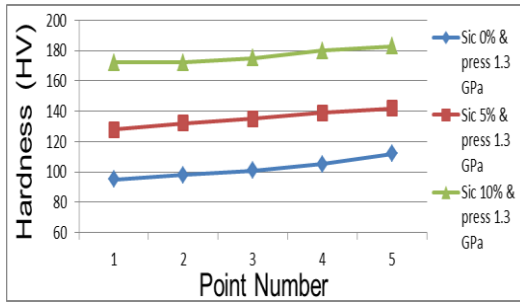


(b) 5%SiC

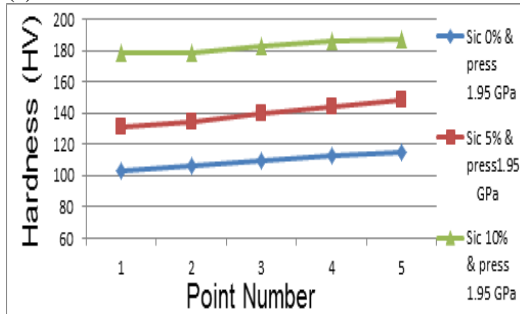


(c) 10% SiC

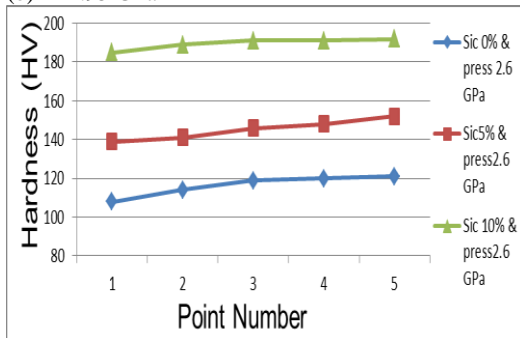
Fig. 16: Vickers hardness measured at 5 points on samples with similar volume fraction of SiC for different compaction pressures



(a) P=1.3 GPa



(b) P=1.95 GPa



(c) P=2.6 GPa

Fig. 17: Vickers hardness measured at 5 points on samples with different levels of SiC for the same compaction pressure

Variation of Vickers and Brinel hardness improvement versus the compaction pressure and the SiC content is illustrated in Figs. 18 and 19, respectively. The hardness given in these figures are the average of the hardness at 5 points shown in Figs. 16 and 17. As it is seen, both figures show more or less the same increase in hardness. The maximum Vickers and Brinel hardness is obtained for the compaction pressure of 2.6 GPa and 10%SiC content. The maximum increases are 100% and 111% for the Vickers and Brinel harnesses, respectively. This is an impressive improvement in the hardness of the compacted specimens. Recently, Atrian et al [33] in a similar work reported an increase of only about 20% in hardness of their compacted samples. The reason for the difference could largely be due to powder oxidation which is a consequence of the compaction where aluminum particles are exposed to oxygen. Atrian et al [33] compacted the powder in air and in this work compaction was performed in an inert atmosphere. The oxidation of aluminum powders causes a hard layer of oxide to be created on aluminum particles. This hard layer prevents a proper inter-bonding of the particles and reduces

the strengthening effects of SiC particles and compaction pressure. This founding shows the importance of the effect of compaction in inert environment. The results are also consistent with those reported by Hubi Haleem et al [13]. They produced aluminum composite reinforced by (3, 6, 9, and 12 wt.%) Al₂O₃ particles using powder technology and prepared the samples by using single action pressing followed directly by sintering process at 500°C under the effect of inert gas conditions. As Figs. 18 and 19 indicate, the enhancement of hardness is due to the effects of compaction pressure and SiC content. A simple calculations shows that the hardness increase due to the compaction pressures of 1.3 GPa to 2.6 GPa for 0%SiC, 5%SiC and 10%SiC is 14%, 7% and 7%, respectively. This is while, the hardness increase due to SiC volume fractions of 0%SiC, 5%SiC and 10%SiC for the pressures of 1.3, 1.96 and 2.9 GPa is 32%, 68% and 63%, respectively.

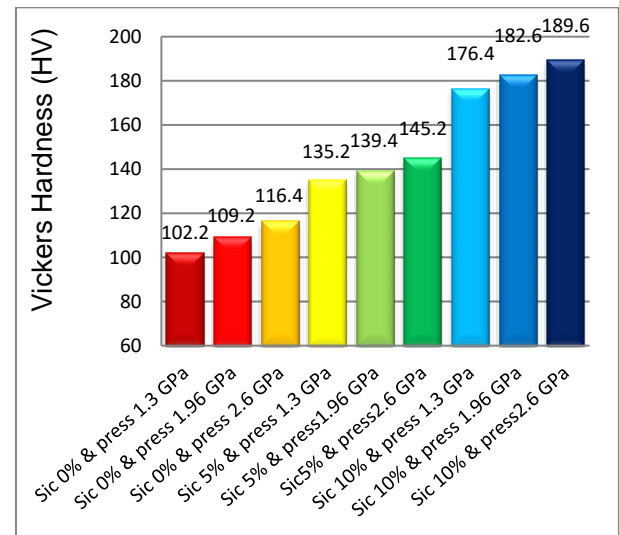


Fig. 18: Variation of Vickers hardness improvement versus the compaction pressure and the SiC particle level

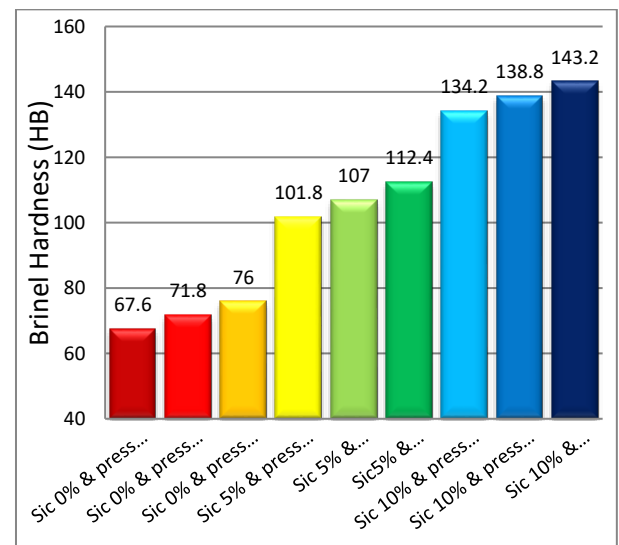


Fig. 19: Variation of Brinel hardness improvement versus the compaction pressure and the SiC particle level

5. CONCLUSIONS

From this study the following conclusions may be derived:

- 1- The compaction of Al7500-SiC powder in an inert atmosphere using a gas such as Nitrogen or Argon significantly improved the mechanical behavior of the compacts.
- 2- The increase of compaction pressure gave rise to the increase of relative density, as expected. The maximum increase with respect to 1.3 GPa pressure was 1.4 and occurred for 2.3 GPa pressure. However, adding the reinforcing SiC particles to aluminum powder exhibited opposite effect and reduced the relative density. The maximum reduction in density was 1.8 and occurred for 10%SiC content.
- 3- In the SiC particles reinforced samples, the porosity increased with the increase of SiC volume fraction. The degree of porosity and the number and size of the void decreased as the compaction pressure increased. The best compaction and the minimum porosity was obtained for the 2.6 GPa compaction pressure.
- 4- The maximum increase in ultimate strength was about 72% and occurred for the 5%SiC content and the 1.3 GPa compaction pressure. For 10%SiC volume fraction the strength improved by 53% for 2.6 GPa pressure. The results showed that the effect of SiC content on ultimate strength was significantly higher than that of the compaction pressure.
- 5- The maximum increases in hardness of the compacts were 100% and 111% for the Vickers and Brinell hardnesses, respectively. These maxima were obtained for the samples with 10%SiC volume fraction compacted at 2.6 GPa pressure. The effect of SiC volume fraction on hardness improvement was found to be remarkably greater than that of compaction pressure.

CONFLICTS OF INTEREST

The authors declare that they have no known competing financial interests or personal relationships that could have appeared to influence the work reported in this paper.

REFERENCES

- [1] J. Gilbert Kaufman, Introduction to Aluminum Alloys and Tempers, ASM International, Materials Park, Ohio, USA, (2000)
- [2] J. E. Hatch (Ed.), Aluminum Properties and Physical Metallurgy, American Society for Metals, OH, (1989).
- [3] John A. Newman, Stephen W. Smith, Robert S. Piascik, K_{max} effects on the near-threshold fatigue crack growth of powder-metallurgy aluminum alloys, International Journal of Fatigue 31 (2009) 1237–1245, <https://doi.org/10.1016/j.ijfatigue.2009.01.002>
- [4] A. Atrian, G.H. Majzoobi, M.H. Enayati, H. Bakhtiari, Mechanical and microstructural characterization of Al7075/SiC nanocomposites fabricated by dynamic compaction. Int J Miner Metall Mater. 21 (2014) 295-303. <https://doi.org/10.1007/s12613-014-0908-7>
- [5] M. Rahimian, N. Parvin and N. Ehsani, Investigation of Particle Size and Amount of Alumina on Microstructure and Mechanical Properties of Al Matrix Composite Made by Powder Metallurgy, Material Science and Engineering A 527 (2010) 1031-1038. <https://doi.org/10.1016/j.msea.2009.09.034>
- [6] M. Gagne, Behavior of Powder Mix Constituents During Cold and Warm Compaction, International Conference on Powder Metallurgy & Particulate Materials, 29 June to 2 July (1997), Chicago, IL
- [7] H. Mirzadeh, A. Najafzadeh, Flow stress prediction at hot working conditions, Mater. Sci. Eng. A 527 (2010) 1160–1164. <https://doi.org/10.1016/j.msea.2009.09.060>
- [8] C. Zubizarreta, S. Gimenez, J.M. Martin, I. Iturriza, Effect of the heat treatment prior to extrusion on the direct hot-extrusion of aluminium powder compacts, Journal of Alloys and Compounds 467 (2009) 191–201. <https://doi.org/10.1016/j.jallcom.2007.12.035>
- [9] M.A. Jabbari Taleghani, E.M. Ruiz Navas, M. Salehi, J.M. Torralba, Hot deformation behaviour and flow stress prediction of 7075 aluminium alloy powder compacts during compression at elevated temperatures, Materials Science and Engineering A 534 (2012) 624– 631. [10.1016/j.msea.2011.12.019](https://doi.org/10.1016/j.msea.2011.12.019)
- [10] M. Jafari, M.H. Abbasi, M.H. Enayati, F. Karimzadeh, Mechanical properties of nanostructured Al2024–MWCNT composite prepared by optimized mechanical milling and hot pressing methods. Adv. Powder Technol. 23 (2012) 205-210. <https://doi.org/10.1016/j.apt.2011.02.008>
- [11] A. Ahmed, A.J. Neely, K. Shankar, P. Nolan, S. Moricca, T. Eddowes, Synthesis, Tensile Testing, and Microstructural Characterization of Nanometric SiC Particulate-Reinforced Al 7075 Matrix Composites. Metall. Mater. Trans. A. 41 (2010) 1582-91. <https://doi.org/10.1007/s11661-010-0201-y>
- [12] A. Alizadeh, E. Taheri-Nassaj, Wear Behavior of Nanostructured Al and Al–B4C Nanocomposites Produced by Mechanical Milling and Hot Extrusion. Tribol Lett. 44 (2011) 59-66. <https://doi.org/10.1007/s11249-011-9825-3>
- [13] Ali Hubi Haleem, Newfal Zuheir, Newal Muhammad Dawood, Preparing and Studying Some Mechanical Properties of Aluminum Matrix Composite Materials Reinforced by Al₂O₃ particles, Babylon university – Materials Engineering Collage, 2011.
- [14] T. Ramesh, M Prabhakar, R Narayanasamy, Workability studies on Al-20%SiC powder metallurgy composite during cold upsetting, International Journal of Advanced Manufacturing Technology 44 (2009) 389-398. <https://doi.org/10.1007/s00170-008-1880-z>
- [15] Ali Kalkanlı, Sencer Yılmaz, Synthesis and characterization of aluminum alloy 7075 reinforced with silicon carbide particulates, Materials and design 29 (2008) 775-780. <https://doi.org/10.1016/j.matdes.2007.01.007>
- [16] D.R. Kumar, C. Loganathan, R. Narayanasamy, Effect of glass in aluminum matrix on workability and strain hardening behavior of powder metallurgy composite, Materials & Design, 32 (2011) 2413–2422. <https://doi.org/10.1016/j.matdes.2010.12.008>

- [17] G. H. Majzoobi, A. Atrian and M. K. Pipelzadeh, Effect of densification rate on consolidation and properties of Al7075-B4C composite powder, *Powder Metallurgy* 58 (2015) 281-288. <https://doi.org/10.1179/1743290115Y.0000000008>
- [18] G.H. Majzoobi, A. Atrian & M.H. Enayati, Tribological properties of Al7075-SiC nanocomposite prepared by hot dynamic compaction, *Composite interfaces* 22 (2015) 579-593. <https://doi.org/10.1080/09276440.2015.1055955>
- [19] A. Atrian, GH. Majzoobi, MH Enayati, H. Bakhtiari, A comparative study on hot dynamic compaction and quasi-static hot pressing of Al7075/SiCnp nanocomposite. *Adv. Powder Technol.* 26 (2015) 73-82. <https://doi.org/10.1016/j.appt.2014.08.007>
- [20] M. Tavoosi, F. Karimzadeh, M. H. Enayati, A. Heidarpour, Bulk Al-Zn/Al₂O₃ nanocomposite prepared by reactive milling and hot pressing methods, *J. Alloys Compd* 475 (2009) 198-201. <https://doi.org/10.1016/j.jallcom.2008.07.049>
- [21] K. Rahmani, G.H. Majzoobi, H. Bakhtiari, A. Sadooghi, On the effect of compaction velocity, size, and content of reinforcing particles on corrosion resistance of Mg-B4C composites, *Materials Chemistry and Physics* 271 (2021) 124946. <https://doi.org/10.1016/j.matchemphys.2021.124946>
- [22] G.H. Majzoobi, K. Rahmani, M. Mohamadi, H. Bakhtiari, R. Das, Tribological behavior of Ti/HA and Ti/SiO₂ functionally graded materials fabricated at different strain rates, *Journal of biotribology* 35-36 (2023) 100233. <https://doi.org/10.1016/j.biotri.2022.100233>
- [23] G.H. Majzoobi, M. Mohammadi, K. Rahmani, Microstructural examination and mechanical characterization of Ti/HA and Ti/SiO₂ functionally graded materials fabricated at different loading rates, *Journal of the Mechanical Behavior of Biomedical Materials* 136 (2022) 105497. <https://doi.org/10.1016/j.jmbbm.2022.105497>
- [24] K. Rahmani, G. H. Majzoobi, H. Bakhtiari, A. Sadooghi, Thermal Properties of Mg-B4C Micro and Nanocomposites Fabricated by Static and Dynamic Compaction Methods, *Trans Indian Inst Met* 75 (2022) 2139-2148. <https://doi.org/10.1007/s12666-022-02590-w>
- [25] R. Cozzens, *Advanced CATIA V5 Workbook Release 16*, SDC Publications; 1st edition 2008.
- [26] J.Z. Wang, X.H. Qu, H.Q. Yin, M.J. Yi, and X.J. Yuan, High velocity compaction of ferrous powder, *Powder Technol.* 192 (2009) 131-136. <https://doi.org/10.1016/j.powtec.2008.12.007>
- [27] A.R. Yazdi, H. Baharvandi, H. Abdizadeh, J. Purasad, A. Fathi, H. Ahmadi, Effect of sintering temperature and siliconcarbide fraction on density, mechanical properties and fracture mode of alumina-silicon carbide micro/nanocomposites, *Mater. Des.* 37 (2012) 251-255. <https://doi.org/10.1016/j.matdes.2011.12.038>
- [28] Y.L. Dong, F.M. Xu, X.L. Shi, C. Zhang, Z.J. Zhang, J.M. Yang, Y. Tan, Fabrication and mechanical properties of nano-/micro-sized Al₂O₃/SiC composites, *Mater. Sci. Eng. A* 504 (2009) 49-54. <https://doi.org/10.1016/j.msea.2008.10.021>
- [29] J.C. Grosskreutz, Fatigue mechanisms in the sub-creep range. *ASTM* (1971). <https://doi.org/10.1520/STP26684S>
- [30] H. Dietmann, *Einführung in die Elastizitäts- und Festigkeitslehre*; Alfred Kröner Verlag: Stuttgart, Germany, 1991
- [31] A. Canakci, Microstructure and abrasive wear behaviour of B4C particle reinforced 2014 Al matrix composites, *Mater Sci* 46 (2011) 2805-2813. <https://doi.org/10.1007/s10853-010-5156-2>
- [32] A. Alizadeh and E. Taheri-Nassaj, Wear Behavior of Nanostructured Al and Al-B4C Nanocomposites Produced by Mechanical Milling and Hot Extrusion, *Tribol Lett* 44 (2011) 59-66. <https://doi.org/10.1007/s11249-011-9825-3>
- [33] A. Atrian, G.H. Majzoobi, M.H. Enayati, H. Bakhtiari, Mechanical and microstructural characterization of Al7075/SiC nanocomposite fabricated by dynamic compaction, *International Journal of Minerals, Metallurgy and Materials* 21 (2014) 295-303. <https://doi.org/10.1007/s12613-014-0908-7>